Linkage Analysis of Susceptibility to Hyperoxia

Nrf2 Is a Candidate Gene

Hye-Youn Cho,* Anne E. Jedlicka, Sekhar P. M. Reddy, Liu-Yi Zhang, Thomas W. Kensler, and Steven R. Kleeberger*

Department of Environmental Health Sciences, Johns Hopkins University, School of Public Health, Baltimore, Maryland

A strong role for reactive oxygen species (ROS) has been proposed in the pathogenesis of a number of lung diseases. Hyperoxia (> 95% oxygen) generates ROS and extensive lung damage, and has been used as a model of oxidant injury. However, the precise mechanisms of hyperoxia-induced toxicity have not been completely clarified. This study was designed to identify hyperoxia susceptibility genes in C57BL/6J (susceptible) and C3H/HeJ (resistant) mice. The quantitative phenotypes used for this analysis were pulmonary inflammatory cell influx, epithelial cell sloughing, and hyperpermeability. Genome-wide linkage analyses of intercross (F_2) and recombinant inbred cohorts identified significant and suggestive quantitative trait loci on chromosomes 2 (hyperoxia susceptibility locus 1 [*Hsl1*]) and 3 (*Hsl2*), respectively. Comparative mapping of *Hsl1* identified a strong candidate gene, *Nfe2l2* (nuclear factor, erythroid derived 2, like 2 or *Nrf2*) that encodes a transcription factor NRF2 which regulates antioxidant and phase 2 gene expression. Strain-specific variation in lung *Nrf2* messenger RNA expression and a T → C substitution in the B6 *Nrf2* promoter that cosegregated with susceptibility phenotypes in F_2 animals supported *Nrf2* as a candidate gene. Results from this study have important implications for understanding the mechanisms through which oxidants mediate the pathogenesis of lung disease.

Incompletely reduced oxygen metabolites can cause cellular damage by oxidizing nucleic acids, proteins, and membrane lipids (1). Reactive oxygen species (ROS) have been implicated in the pathogenesis of many acute and chronic clinical disorders, such as adult respiratory distress syndrome, bronchopulmonary dysplasia (BPD), ischemia-reperfusion injury, atherosclerosis, neurodegenerative diseases, and cancer (2). The lung is particularly at risk to the toxic effects of ROS because it interfaces with various oxidants, such as environmental pollutants and cigarette smoke.

Characteristic features of oxidative lung disease have been reproduced in laboratory animals by exposure to hyperoxia (> 95% oxygen). Hyperoxia generates ROS in the lungs of animals (3), and causes extensive pulmonary damage characterized by inflammation and death of capillary endothelial and alveolar epithelial cells that result in pulmonary edema and severe impairment of respiratory functions (4, 5). Sufficiently long (≥ 3 d) exposure to hyperoxia is lethal (6). Although the precise molecular mechanisms by which hyperoxia produces lung injury remain unresolved, excess production of ROS that could overwhelm endogenous antioxidant defenses has been proposed (7).

The time course and severity of injury induced by hyperoxia varies as a function of age, gender, and genetic background (8–11). Significant interstrain variation in response to hyperoxic lung injury has been reported in rodents. Greater sensitivity to hyperoxia occurs in Fischer rats compared with Sprague–Dawley (12, 13) and, among inbred mice, the C57BL/6J (B6) strain has greater pulmonary inflammation and injury to hyperoxia challenge than does the C3H/HeJ (C3) strain (14–16). However, the precise genetic basis for the interstrain differences has not been identified.

In the present study, we determined chromosomal loci of susceptibility genes that control hyperoxia-induced pulmonary injury in mice. Genome-wide screens with BXH recombinant inbred (RI) strains and a $B6C3F_2$ cohort identified significant and suggestive susceptibility quantitative trait loci (QTLs) on chromosomes 2 and 3, respectively.

A candidate gene within the chromosome 2 QTL is *Nfe2l2* (nuclear factor [NF], erythroid derived 2, like 2 or *Nrf2*), which encodes a transcription factor NRF2 (NF-E2 related factor 2). Recently, NRF2 has been identified as an antioxidant response element (ARE)–mediated positive regulator of detoxifying enzyme genes for protecting cells against electrophile toxicity, oxidative stress, and carcinogenicity (17–21). Further, mice with site-directed mutation (knockout) of *Nrf2* ($Nrf2^{-/-}$) were found to have significantly enhanced responsiveness to hyperoxia relative to wild-type mice ($Nrf2^{+/+}$) (22). To begin testing the hypothesis that *Nrf2* is a candidate gene for differential susceptibility to oxygen toxicity in B6 and C3 mice, hyperoxia-induced *Nrf2* messenger RNA (mRNA) expression was evaluated in the lungs of both mouse strains. Sequence analysis of *Nrf2* from B6 and C3 mice was also done to identify the potential molecular basis for differential susceptibility to hyperoxic pulmonary injury.

Materials and Methods

Animals

B6, C3, $B6C3F_1/J$ (F_1) hybrid, and BXH RI mice (6 to 8 wk) were purchased from Jackson Laboratories (Bar Harbor, ME). All animals were housed in a virus- and antigen-free room. Water and mouse chow were provided *ad libitum.* Cages were placed in laminar flow hoods with high-efficiency particulate-filtered air. Sen-

(*Received in original form February 21, 2001 and in revised form May 24, 2001*)

Address correspondence to: Steven R. Kleeberger, Ph.D., Div. of Physiology, Rm. 7006, Johns Hopkins University, 615 N. Wolfe St., Baltimore, MD 21205. E-mail: skleeber@jhsph.edu

**Current address:* Laboratory of Pulmonary Pathobiology, National Institute of Environmental Health Sciences, Research Triangle Park, NC 27709.

Abbreviations: antioxidant response element, ARE; bronchoalveolar lavage, BAL; Bal fluid, BALF; base pair(s), bp; bronchopulmonary dysplasia, BPD; complementary DNA, cDNA; γ-glutamylcysteine synthetase, GCS; glutathione-S-transferase, GST; heme-oxygenase-1, HO-1; hyperoxia susceptibility locus, *Hsl*; interleukin, IL; messenger RNA, mRNA; nuclear factor, NF; nitric oxide, NO; nicotinamide adenine dinucleotide phosphate:quinone oxidoreductase 1, NQO1; NF, erythroid derived 2, like 2, *Nrf2*; polymerase chain reaction, PCR; polymorphonuclear leukocyte, PMN; quantitative trait locus, QTL; restriction fragment-length polymorphism, RFLP; recombinant inbred, RI; reactive oxygen species, ROS; reverse transcriptase, RT; simple sequence-length polymorphism, SSLP.

Am. J. Respir. Cell Mol. Biol. Vol. 26, pp. 42–51, 2002
Internet address: www.atsjournals.org

tinel animals were examined periodically (titers and necropsy) to ensure that the animals remained free of infection. All experimental protocols conducted in the mice were carried out in accordance with the standards established by the U.S. Animal Welfare Acts, set forth in NIH guidelines and the Policy and Procedures Manual (Johns Hopkins University School of Public Health Animal Care and Use Committee).

Breeding Studies

$B6C3F_1$/J mice were intercrossed to produce $B6C3F_2$ progeny in our animal facilities. Progeny were weaned at 3 to 4 wk of age, separated according to gender, and housed in microisolation cages until they reached the appropriate age for experimentation (6 to 8 wk).

Oxygen Exposure

Mice were placed on a fine mesh wire flooring in a sealed 45-l glass exposure chamber. The chamber bottom was lined with CO_2 absorbent (Soda-sorb; WR Grace, Lexington, MA). Water and mouse chow were provided *ad libitum.* Humidified pure oxygen or air was delivered to the chamber at a flow rate of 7 liters/min, sufficient to provide 10 changes/h. The concentration of oxygen in the exhaust from the chamber was monitored (Beckman OM-11; Beckman Instruments, Irvine, CA) throughout the experiments. The oxygen concentration for all experiments ranged from 95 to 99%. The chambers were opened once a day for 10 min to replace CO_2 absorbent, food, and water.

Bronchoalveolar Lavage and Phenotyping

Immediately after exposure, mice were removed from the chamber, weighed, and anesthetized with sodium pentobarbital (104 mg/kg). Assessment of pulmonary inflammation and injury was done using bronchoalveolar lavage (BAL). Lungs were lavaged four times *in situ* with Hanks' balanced salt solution (HBSS) (35 ml/kg, pH 7.2–7.4). Recovered BAL fluid (BALF) from each mouse was immediately cooled to 4°C. For each mouse, the four BAL returns were centrifuged (500 × *g*, 4°C), and the supernatant from the first BAL return was decanted for determination of total protein (an indicator of lung permeability). Protein concentration was measured following the method of Bradford (23). The cell pellets from all lavage returns were combined and resuspended in 1 ml of HBSS. The numbers of cells (per ml total BAL return) were counted with a hemocytometer as indicators of lung injury and inflammation. An aliquot (200 μl) of BAL return cell suspension was cytocentrifuged (Shandon Southern Products, Pittsburgh, PA), and stained with Wright–Giemsa stain (Diff-Quik; Baxter Scientific Products, McGaw Park, IL) for differential cell analysis. Differential counts for epithelial cells, macrophages, and polymorphonuclear leukocytes (PMNs) were done by identifying 300 cells according to standard cytologic techniques (24). Epithelial cells in particular were identified by the presence of cilia.

DNA Extraction and Genotyping

DNA was extracted from a kidney of each phenotyped F_2 animal and prepared for polymerase chain reaction (PCR). PCR reactions were run in 96-well plates following standard conditions as previously described (25). Primers for simple sequence-length polymorphisms (SSLPs) that differed between B6 and C3 progenitors (i.e., informative for linkage mapping) were purchased from Research Genetics (Huntsville, AL).

Genetic Linkage Analyses

Linkage analyses were initiated in the F_2 cohort by scanning the entire genome for associations between SSLPs and hyperoxia response phenotypes in 25 selected high-responder and nonresponder F_2 mice (i.e., selective genotyping [26, 27]). Interval analyses were performed on the F_2 data set by fitting regression equations for the effects of hypothetical QTLs at the position of each SSLP marker and at 1-cM intervals between SSLPs. The dominance properties of each putative QTL were evaluated by performing interval analyses using free, additive, recessive, and dominant regression models. The regressions and significance of each association (likelihood ratio χ^2 statistic) were calculated by the Map Manager QTb27 program, which is distributed electronically and available at http://mcbio.med.buffalo.edu/mmQT.html (28). Putative QTLs identified in the selected F_2 mice were further analyzed by including the entire cohort and additional markers within the chromosomal interval identified by selective genotyping. Permutation tests were performed on the phenotype and genotype data to establish empirically the significance thresholds of all QTL mapping results (Map Manager QTb27 and following methods of Churchill and Doerge, ref. 29). For the genome scan, 10,000 permutations were performed to establish significant and suggestive linkage threshold values. These values correspond to the genome-wide probabilities proposed by Lander and Kruglyak (30). To conform to assumptions of the linkage analyses, BALF protein concentration and cell data were tested for normality and homoscedasticity.

A second, independent, genome-wide search for QTLs was done using the mean hyperpermeability and cell response phenotypes for each RI strain in the BXH RI set. Interval analyses were done as described for the F_2 cohort using markers in the strain distribution library. Only the additive regression model was used for the RI analyses. The markers used in these analyses have been typed for the BXH RI strains by numerous investigators and are archived in Map Manager (28). Permutation tests and analysis for linkage were performed as described earlier.

Nrf2 mRNA Expression in Lung

Total RNA was isolated from left lung following Chomczynski and Sacchi (31) and as indicated in the Trizol (Life Technologies, Gaithersburg, MD) reagent specifications. *Nrf2* expression was analyzed by reverse transcriptase (RT)–PCR. Briefly, 500 ng of pooled RNA from mice of each group (n = 3/group) was reverse transcribed into complementary DNA (cDNA) in a volume of 50 μl. Reactions contained 1× PCR buffer (50 mM KCl and 10 mM Tris, pH 8.3), 5 mM $MgCl_2$, 1 mM each deoxynucleotide triphosphates (dNTPs), 125 ng oligo (dT), and 50 U of Moloney murine leukemia virus RT (Life Technologies). PCR was performed with an aliquot of cDNA (10 μl) at a final concentration of 1× PCR buffer, 2 mM $MgCl_2$, 400 μM dNTPs, and 1.25 U *Taq* polymerase in a total volume of 25 μl using 240 nM each of forward and reverse primers specific for mouse *Nrf2* (5′-ATGGATTTGATTGACATC CTT-3′, 5′-CTAGTTTTTCTTTGTATCTGG-3′) and *Actb* (5′-GTG GGCCGCTCTAGGCACCA-3′, 5′-CGGTTGGCCTTAGGGTTC AGG-3′) as an internal control. PCR was started with 5 min incubation at 94°C followed by a three-step temperature cycle; denaturation at 94°C for 30 s, annealing at 57°C for 30 s, and extension at 72°C for 1 min for 25 to 30 cycles. A final extension step at 72°C for 10 min was included after the final cycle. The number of cycles was chosen to ensure that amplification product did not reach a plateau level. PCR products were separated on ethidium bromide–stained 1.2% agarose gel. Digitized images of *Nrf2* cDNA bands were quantitated using a Bio-Rad Gel Doc 2000 Analysis System (Bio-Rad Laboratories, Hercules, CA), and the ratio of *Nrf2* cDNA to *Actb* cDNA was determined and presented.

Nrf2 Sequence Analysis

Sequence variations in *Nrf2* between B6 and C3 mice were determined using primers that span the 1-kb promoter and 2.3-kb coding regions. Primers were designed from the published sequences

TABLE 1

Total protein concentration (μg/ml) and numbers ($\times 10^3$/ml) of PMNs and macrophages recovered in BALF from BXH RI mice after exposure to 100% oxygen

Strain or RI*	Total Protein	PMNs	Macrophages
RI #2 (5)	612 ± 70	12.0 ± 2.4	90.0 ± 6.7
3 (5)	1,118 ± 260	2.2 ± 0.3	75.4 ± 7.8
4 (5)	1,247 ± 218	6.6 ± 0.7	66.6 ± 7.6
6 (6)	748 ± 81	1.5 ± 0.3	96.0 ± 9.8
7 (6)	1,512 ± 138	13.0 ± 1.6	53.2 ± 8.3
8 (5)	318 ± 56	3.3 ± 0.8	114.6 ± 19.1
9 (5)	1,627 ± 108	4.2 ± 1.6	80.0 ± 8.8
10 (5)	2,500 ± 225	1.5 ± 0.3	48.9 ± 7.5
11 (5)	1,155 ± 175	3.6 ± 0.8	80.8 ± 5.0
12 (6)	1,209 ± 192	12.3 ± 2.6	85.4 ± 5.0
14 (5)	942 ± 198	3.4 ± 1.3	92.1 ± 8.3
19 (5)	595 ± 98	7.4 ± 2.4	84.3 ± 7.8

*Number in parentheses is sample size.
†Means ± standard error of the mean.

of Chan and colleagues for mouse *Nrf2* promoter (GenBank U70474) and cDNA (32). PCR conditions were optimized using the Fail Safe PCR system (Epicentre Technologies, Madison, WI) to yield a single, specific product of high concentration from which multiple sequencing reactions were run using internal primers. ABI-Prism fluorescent methods and reagents were used for subsequent analysis on an ABI 377 Automated DNA sequencer (Applied Biosystems, Foster City, CA). Resultant sequences of each strain were aligned and compared with the published sequences derived from the 129/SvJ strain (GenBank U70474). Polymorphisms between B6 and C3 mice were confirmed by repeat and/or overlapping sequence reads, and by analysis of $B6C3F_1$/J mice to demonstrate heterozygosity. Polymorphisms were analyzed by MacVector 5.0 (IBI) to determine whether an alteration in the restriction profile of the segment occurred, enabling development of a restriction fragment-length polymorphism (RFLP) assay.

RFLP for the *Nrf2* −336 Promoter Polymorphism

Primers were designed to amplify a 326–base pair (bp) fragment of the promoter, from bp −93 to −419. Digestion of the PCR product with restriction enzyme *Bsu36 I* (New England Biolabs, Beverly, MA) cut uniquely at the −336 site in C3 mice resulting in two fragments, or bands, of 242 and 84 bp. In B6 mice, which possess a T → C substitution (*see* RESULTS), the site is abolished, therefore resulting in the presence of only the full-length, 326-bp fragment on the gel. In C3 mice and F_1 mice, two (fragmented 242 and 84 bp) and three bands (intact 326, and fragmented 242 and 84 bp) were resolved, respectively. Bands were easily resolved and heterozygous F_1 and F_2 animals were distinguishable and genotyped accordingly.

Lung Tissue Preparation for Histopathology

Left-lung tissues from air- and hyperoxia (72 h)-exposed B6 and C3 mice were fixed with zinc formalin, embedded in paraffin, and sectioned 5 μm thick. Tissue sections were histochemically stained with hematoxylin and eosin (H&E) for morphologic evaluation of pulmonary injury.

Statistics

Linear regression was used to assess the relationship between hyperoxia response phenotypes (BALF protein and cells) in F_2 ani-

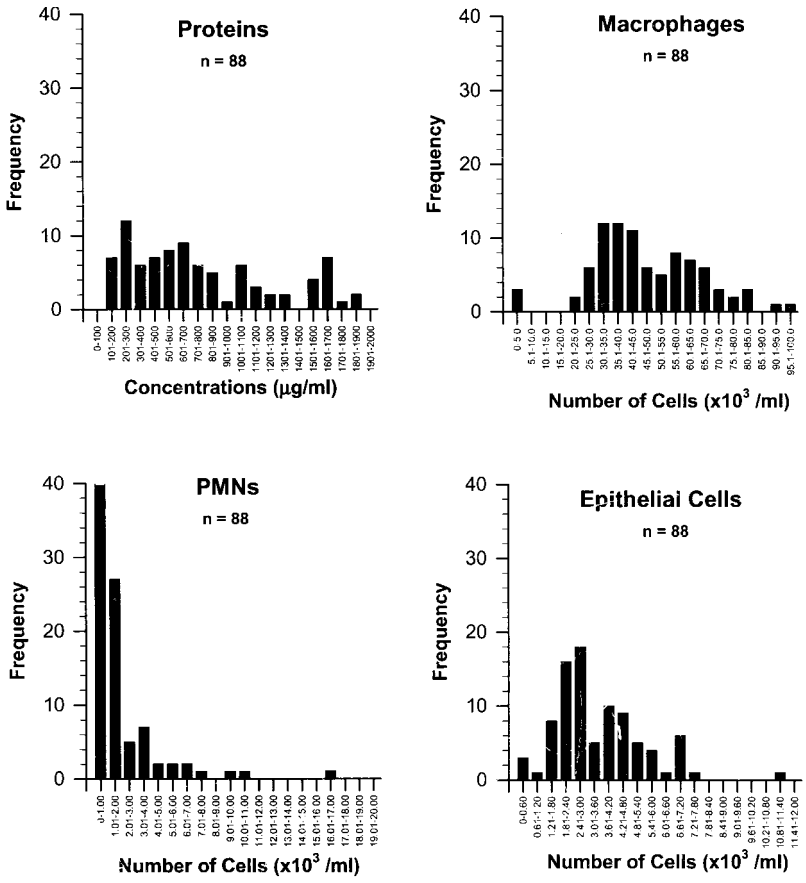

Figure 1. Frequency distribution of the concentration (μg/ml) of proteins and the number ($\times 10^3$/ml) of macrophages, PMNs, and epithelial cells in BALF recovered from $B6C3F_2$ mice after 72 h exposure to 100% oxygen.

mals (n = 88). Data sets were tested for homoscedasticity as required for parametric analyses, and data that did not meet this requirement (i.e., heteroscedastic) were transformed (ln or arcsine). The analysis was performed using a commercial statistical analysis package (SigmaStat; Jandel Scientific Software, San Rafael, CA). Statistical significance was accepted at $P < 0.05$.

Results

Hyperoxia Phenotypes in B6C3F$_2$ and BXH RI Mice

BXH RI (Table 1) and F_2 mice were exposed to 100% oxygen for 72 h and phenotyped for changes in total protein (a marker of lung permeability) and inflammatory and endothelial cells recovered by BAL. The frequency–response distribution of each phenotypic parameter in the F_2 animals (Figure 1) was within the ranges of similarly exposed B6 and C3 mice. Linear regression analysis was used to determine whether the response phenotypes cosegregated in the F_2 mice. Statistically significant correlations ($P < 0.05$) were found between numbers of epithelial cells and inflammatory cells (*i.e.*, PMNs and macrophages), and between the numbers of inflammatory cells (Figure 2). Interestingly, no correlation was found between BALF protein and any of the cell types.

Genetic Linkage Analyses

A genome-wide search for QTLs was initially performed with 25 selected high-responder ($n = 13$) and nonresponder ($n = 12$) mice from an F_2 cohort (selective genotyping; refs. 26 and 27) genotyped at 117 SSLPs. Suggestive QTLs were identified on chromosomes 2 and 3 (Figure 3). Potentially important linkages were also found on chromosomes 1, 4, and 11 (Figure 3). The putative QTLs on chromosomes 2 and 3 were analyzed further by including the entire F_2 cohort (n = 88 mice, 176 meioses) and 18 additional SSLPs. Interval mapping confirmed a susceptibility locus for macrophage, epithelial cell, and PMN phenotypes on chromosome 2 between *D2Mit271* and *D2Mit476* (Figure 4). The χ^2 value for the QTL with PMNs (13.2) exceeded the threshold value for statistically significant linkage and approached the threshold for highly significant linkage (Figure 4A). The χ^2 values for linkage of macrophage (6.9) and epithelial cell (10.7) responses to the same interval also exceeded the suggestive linkage threshold (5.5 and 3.3, respectively) (Figures 4B and 4C). Statistical association ($\chi^2 = 9.7$) of the chromosome 3 QTL with the protein phenotype exceeded the suggestive linkage threshold (5.7), but did not reach statistical significance (13.9) (data not shown). In this model, the observed peaks in the QTLs associate with the B6 allele. We have designated the chromosome 2 QTL as hyperoxia susceptibility locus (*Hsl*) *1* and the chromosome 3 QTL as *Hsl2.* Composite interval mapping was done to determine the potential influence of *Hsl2* on *Hsl1.* When *Hsl2* was controlled, the χ^2 value of *Hsl1* did not change, which suggested that the two QTLs were independent. The total trait variance explained by *Hsl1* between *D2Mit37* and *D2Mit94*, which has the highest likelihood ratio statistics in the QTL, was approximately 42%. The total trait variance explained by *Hsl2* at *D3Mit266* and *D3Mit43* was approximately 13%. A second, independent genome scan for susceptibility loci was done using the BXH RI set. Associations were tested between the quantitative hyperoxia response phenotypes and 558 SSLPs and other polymorphic markers that have been typed for the BXH RI strains (28). Interval analyses identified suggestive QTLs on chromosomes 2 and 3 that overlapped those identified by the F_2 cohort analysis (Table 2).

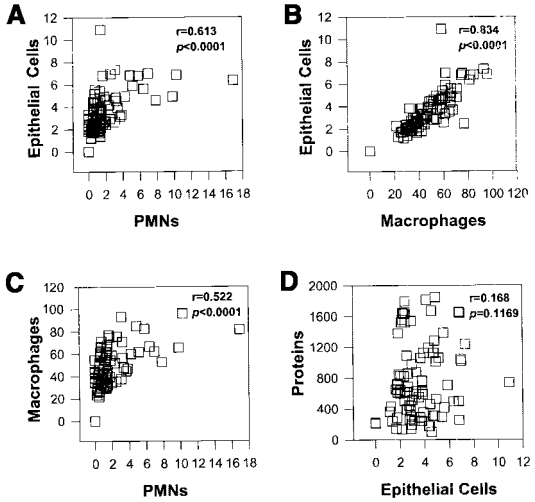

Figure 2. Cosegregation plots of the number ($\times 10^3$/ml BAL return) of epithelial cells versus PMNs (*A*), epithelial cells versus macrophages (*B*), macrophages versus PMNs (*C*), and proteins (μg/ml BAL return) versus epithelial cells (*D*) recovered from B6C3F$_2$ mice after 72 h exposure to 100% oxygen. r = correlation coefficient. *Symbols* represent responses from each B6C3F$_2$ animal. Group size is 88 for each panel.

Nrf2 mRNA Expression

Comparative mapping of *Hsl1* between *D2Mit37* and *D2Mit382* identified a candidate susceptibility gene, *Nrf2*, which is known to regulate the expression of several antioxidant and phase 2 enzyme genes bearing ARE in their 5′ upstream promoter region. Previous work from our laboratory has determined that targeted disruption of *Nrf2* significantly enhanced susceptibility to hyperoxic lung injury in mice (22). To examine the putative role of *Nrf2* in differential hyperoxia susceptibility in the current study, we first determined *Nrf2* mRNA expression kinetics in B6 and C3 mice by RT-PCR. Basal *Nrf2* mRNA levels in the lungs were approximately 1.8-fold higher in C3 mice than in B6 mice (Figure 5A). Hyperoxia increased *Nrf2* mRNA expression slightly over the basal levels as early as 1.5 h in both strains. The induced mRNA levels remained elevated in C3 mice by 48 h exposure, and increased again at 72 h. *Nrf2* mRNA levels decreased below basal expression in B6 mice at 24 h exposure, and remained depressed by 48 h. A marked increase similar to C3 mice was observed after 72 h of exposure. The induced levels of *Nrf2* mRNA were 62 to 64% greater in C3 mice than in B6 mice at 1.5 and 6 h, and were 2.6-fold greater at 48 h. No difference in *Nrf2* mRNA levels was detected between B6 and C3 mice at 72 h.

Sequence Analysis of *Nrf2*

Sequence analysis of the *Nrf2* promoter in B6 and C3 mice revealed several variations between each other and the published sequence (129/SvJ) used for our comparisons (32). B6

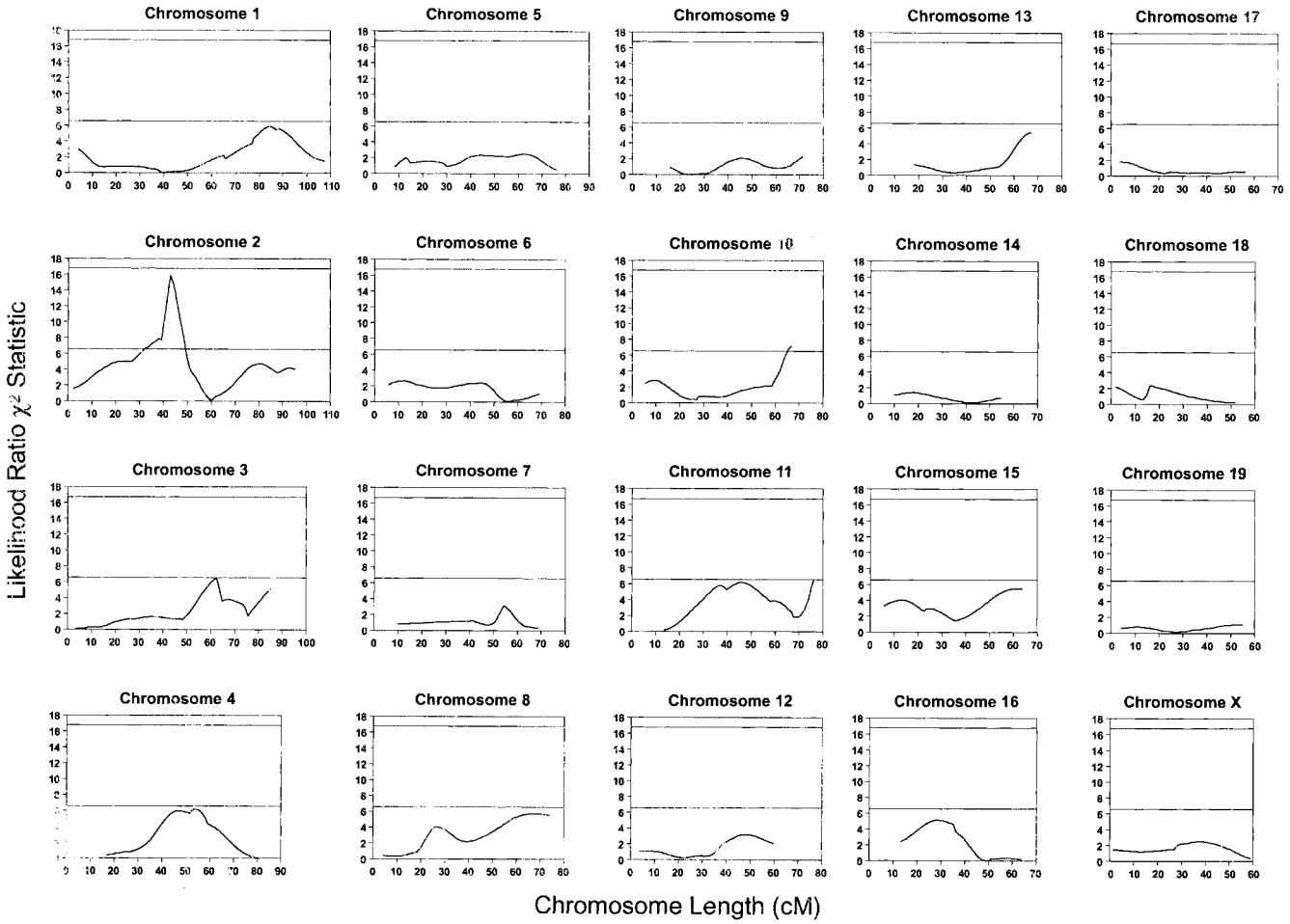

Figure 3. A genome-wide search for QTLs by selective genotyping of the B6C3F_2 cohort. The *x*-axis for each plot is the length of the chromosome in centimorgans (cM). The *y*-axis is the likelihood ratio χ^2 statistic. The significance of each association (likelihood ratio χ^2 statistic) was calculated by Map Manager QTb27. To establish empirically the significance thresholds of all QTL mapping results, permutation tests were performed using Map Manager and following methods of Churchill and Doerge (29). A total of 10,000 permutations were performed to establish significant and suggestive linkage threshold values. These values corresponded to the genome-wide probabilities proposed by Lander and Kruglyak (30). The *upper* and *lower horizontal lines* in each plot represent significant and suggestive linkage thresholds, respectively.

mice possess a G → C substitution at −89, and have T → C substitutions at −197, −336, and −479. B6 mice also have an additional C within a poly-C tract at −519; in C3 mice the C repeat extends only to − 518. C3 mice have a T → A substitution at −1,040. B6 and C3 both possess an A → C substitution at −241 and a six-bp deletion from −454 to −459 compared with 129/SvJ.

Putative transcription factor binding sites within this entire region, and potential alterations resulting from such variations between strains, were analyzed using the TFSEARCH program (http://pdap1.trc.rwcp.or.jp/research/db/TFSEARCH.html). The −336 polymorphism (Figure 5B) is predicted to add a Sp1 transcription factor-binding site in B6 mice compared with C3. To determine whether the polymorphism segregated with susceptibility phenotype, we designed an RFLP assay to genotype B6C3F_2 mice. Within a 326-bp amplified segment of the promoter, the restriction enzyme *Bsu36 I* cut uniquely at the −336 site in C3 mice, and enabled resolution of B6 and C3 genotypes (Figure 5C). The −336 RFLP genotypes of the F_2 mice cosegregated with informative SSLP genotypes (*D2Mit248* and *D2Mit94*) at the peak of *Hsl1* QTL and located 1-cM distal to *Nrf2* locus (46 cM). The −336 polymorphism was also significantly linked with the hyperoxia-induced inflammatory and permeability phenotypes in the F_2 cohort ($\chi^2 = 13.5$) (*see* Figure 4A).

Three polymorphisms were found in the entire coding and 3′ untranslated regions of *Nrf2* in cDNAs from B6, C3, and B6C3F_1/J mice. C3 mice have a T → C substitution at bp 211, a C → T substitution at 271, and a G → A substitution at 1,021, compared with B6 mice. However, the corresponding amino acids Phe71, His91, and Thr341, respectively, remain unaltered.

Lung Histopathology

No significant pathology was observed in lungs of air-exposed B6 (Figure 6A) and C3 (Figure 6B) mice as assessed by light microscopy. The lungs were normal, with regularly shaped alveoli. However, hyperoxia-exposed B6

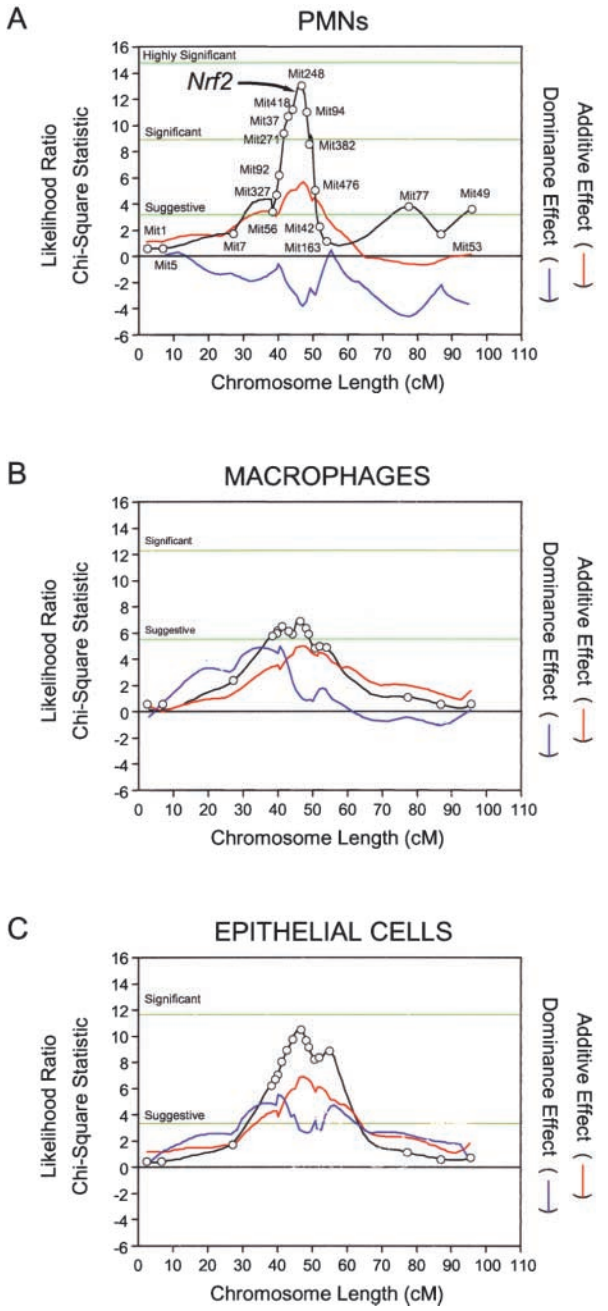

Figure 4. Plots of the likelihood ratio χ^2 statistic (*black*), additive regression coefficient (*red*), and dominance regression coefficient (*blue*) for the association of hyperoxia-induced changes in PMNs (*A*), macrophages (*B*), and epithelial cells (*C*) with polymorphic SSLP markers (*open circles*) on chromosome 2 in B6C3F$_2$ animals. The χ^2 statistic (*y*-axis) is plotted against the markers in the correct order and genetic distance (*x*-axis). The regressions and significance of each association (likelihood ratio χ^2 statistic) were calculated by Map Manager QTb27. Highly significant, significant, and suggestive linkage thresholds were determined by permutation test and are presented (*green lines*). Linkage of the *Nrf2* promoter polymorphism (*see* RESULTS) with hyperoxia susceptibility is indicated in *A*.

TABLE 2

Descriptive statistics for suggestive QTLs identified by BXH RI analysis of three response phenotypes for hyperoxic lung injury

Phenotype	Chromosome	Approximate Position (cM)*	Peak χ^2 Statistic†	*P* Value
Macrophages	2	45.0	15.4	0.00009
	3	71.2	8.0	0.00470
PMNs	3	8.0	16.6	0.00005
Total Protein‡	2	33.0	10.0	0.00155
	3	26.4	13.7	0.00022
	3	53.7	7.0	0.00080

*The approximate center of the QTL.
†Likelihood ratio χ^2 statistic for linkage.
‡A marker of lung permeability.

mice had diffuse and extensive lung parenchymal injury, mainly characterized by severe intra-alveolar plasma exudates and cellular debris; macrophage (predominant) and PMN infiltration in interstitial, alveolar, perivascular, and air spaces; alveolar epithelial cell necrosis; and sloughing of cells (Figures 6C and 6E). Congestion (increases in the number of red blood cells), thickening of alveolar septum, and perivascular swelling were also observed throughout the lungs of B6 mice after hyperoxia exposure (Figures 6C and 6E). Destruction of alveolar structure was obvious in these animals. In contrast, moderate epithelial necrosis, intra-alveolar exudates and cellular debris, inflammation, and thickening of alveolar septum were noted in the lungs of hyperoxia-exposed C3 mice (Figures 6D and 6F). The pathology in these mice was scattered and focal.

Discussion

Evidence supporting the role of genetic predisposition to hyperoxic lung injury can be inferred from the experience with BPD in premature infants supplemented with oxygen. Increased incidence of BPD among infants with the HLA-A2 haplotype has been demonstrated (33). Data from a twin study in which BPD status of the first twin remained a highly significant predictor of BPD in the second twin also implied possible genetic influence in the development of BPD (34). Genetic influence on oxygen toxicity is also supported by interstrain variation in timing and appearance of hyperoxic lung injury among inbred mice (10, 11, 14–16) and rats (12, 13). Previous genetic analyses of pulmonary responses to hyperoxia in our laboratory suggested that susceptibility is not inherited as a Mendelian trait (14), i.e., the responses are quantitative or multigenic. In the present study, independent genome-wide linkage analyses with RI strains and F$_2$ mice identified hyperoxia susceptibility QTLs on mouse chromosomes 2 (*Hsl1*) and 3 (*Hsl2*). This is the first demonstration that specific genetic loci play key roles in differential pulmonary responses to hyperoxia.

Comparative mapping of *Hsl1* identified *potential* candidate susceptibility genes, including *Itga4* (integrin alpha 4), *Itgav* (integrin alpha V), *Chrm4* (cholinergic receptor, muscarinic 4), *Prkar1b-rs* (protein kinase, cyclic adenosine monophosphate–dependent regulatory), and *Nrf2.* However, with the exception of *Nrf2*, there is currently little

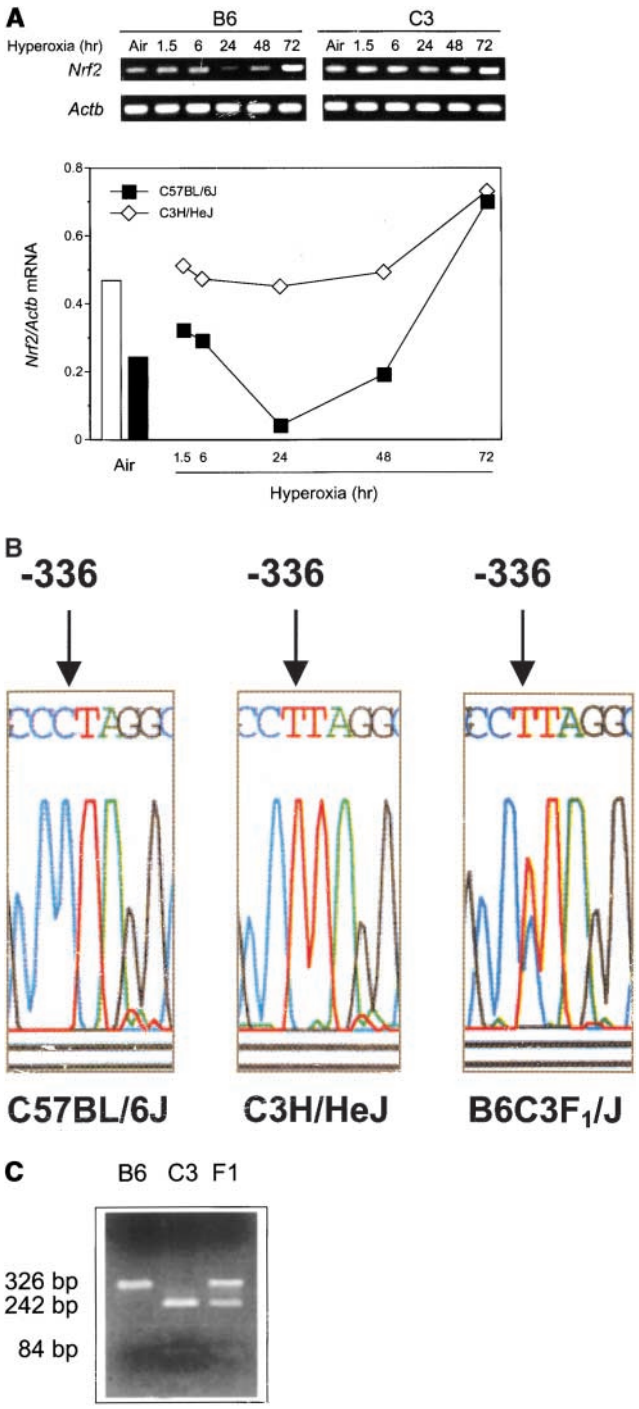

Figure 5. Detection of strain-specific variation in lung *Nrf2* mRNA expression (A) and polymorphism in *Nrf2* promoter sequence (*B* and *C*). (*A*) Changes of *Nrf2* mRNA expression in B6 and C3 mice after 1.5, 6, 24, 48, and 72 h exposure to hyperoxia. (*B*) Sequence chromatographs from the *Nrf2* promoter of B6, C3, and $B6C3F_1/J$ mice showing a T → C substitution at position −336 that is predicted to add a Sp1 binding site in B6 mice. (*C*) RFLP for the T → C substitution at −336 in B6, C3, and $B6C3F_1$ (F1) mice.

evidence to support any of these genes in oxidative lung injury. NRF2 is a cap'n'collar-basic region leucine zipper transcription factor originally detected in erythroid cells but is expressed abundantly in murine liver, intestine, lung, and kidney, where detoxification reactions occur routinely (32). Because of high similarity between the NRF2-binding sequence (NF-E2 motif) and the ARE in regulatory regions of several phase 2 detoxifying enzymes (e.g., nicotinamide adenine dinucleotide phosphate:quinone oxidoreductase 1 [NQO1]; glutathione-S-transferases [GSTs]) (20), NRF2 has been proposed as a putative mediator of ARE responses. Recent studies using *Nrf2*-knockout mice and *Nrf2*-transfected or -deficient cell lines revealed that NRF2, in association with other transcription factors such as c-Jun and small Maf, played an essential role in ARE-mediated induction of protective phase 2 enzymes including NQO1, GST, or γ–glutamylcysteine synthetase (GCS) and heme-oxygenase-1 (HO-1) (17–19, 21, 35). Further, a recent study by Chan and Kan (36) showed that *Nrf2*-knockout mice exposed to butylated hydroxytoluene (BHT) had lower levels of RNA transcripts for classical antioxidant enzymes including superoxide dismutase (SOD) 1 and catalase as well as phase 2 enzymes including NQO1 and GCS in lungs. *Nrf2*-knockout mice were also more susceptible to acute lung injury than were similarly exposed wild-type mice. In contrast to oxidative toxicity induced by hyperoxia, BHT is metabolically activated to reactive quinone methide derivatives, which are thought to mediate its cytotoxic action (37). *Nrf2*-knockout mice also show high sensitivity to acetaminophen hepatotoxicity (38) and benzo[a]pyrene gastric carcinogenesis (39).

Classical antioxidants, including SODs, catalase, and glutathione reductase, have been relatively well documented as defense enzymes against hyperoxic pulmonary injury (e.g., 40, 41). Although limited information is available, investigators have also suggested indirect antioxidant roles of several phase 2 detoxifying enzymes in oxidative injury models (42, 43). In pulmonary tissues (44) or cells (45), enhanced mRNA expression of NQO1 and GCS concomitant with increased enzyme activities were elicited by oxidant exposure (e.g., hyperoxia, hydrogen peroxide). In addition to the phase 2 enzymes, HO-1 was determined as an important enzyme in the pulmonary protection against hyperoxic lung injury in rats (46). We recently determined that *Nrf2*-deficient mice with attenuated basal and/or induced mRNA expression of several phase 2 enzymes (e.g., NQO1, GST-Ya) and HO-1 are significantly more susceptible to inflammatory and hyperpermeability responses to hyperoxia exposure compared with wild-type mice (22). Further, Ishii and coworkers (47) demonstrated that peritoneal macrophages isolated from *Nrf2*-knockout mice have impaired induction of oxidative stress–inducible proteins (e.g. HO-1; A170, peroxiredoxin MSP23), which enhanced susceptibility to electrophiles and oxidants. Our linkage results, as well as these previous reports, led us to hypothesize that defects or alterations in the expression and/or activity of *Nrf2* lead to decreased production of ARE-regulated antioxidant/defense enzymes in the lung, and cause greater sensitivity of the susceptible mice to hyperoxic pulmonary injury.

Sequence analysis of the *Nrf2* promoter in B6 and C3 mice identified a T → C substitution at the −336 position that is predicted to cause an additional Sp1 binding site in B6 mice. Importantly, this polymorphism cosegregated in the F_2 cohort with hyperoxia susceptibility and informative SSLPs in *Hsl1*. Sp1, together with NF-κB and activa-

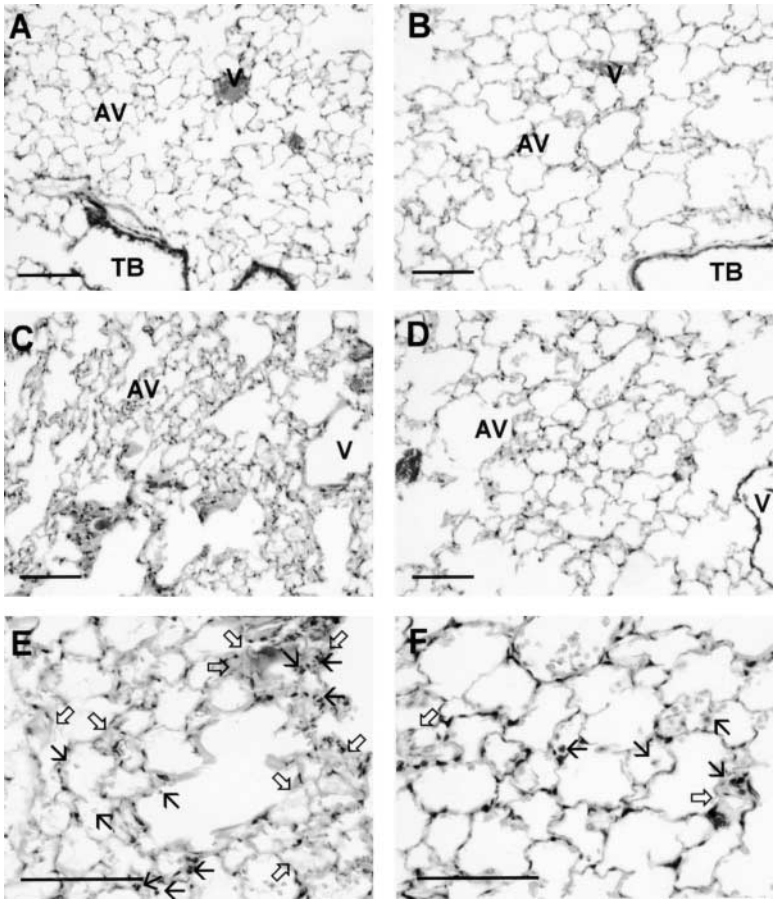

Figure 6. Light photomicrographs of lungs from room air-exposed B6 (*A*) and C3 (*B*) mice, or from hyperoxia (72 h)-exposed B6 (*C* and *E*) and C3 (*D* and *F*) mice. Higher magnification (*E* and *F*) was applied to mice exposed to hyperoxia for better visualization of lung injury. Tissue sections were stained with H&E. *Bar* = 100 μm. AV, alveoli; TB, terminal bronchiole; V, blood vessel; *thin arrow*, inflammatory cells; *thick arrow*, exudates.

tor protein-1, is known as a redox-sensitive transcription factor. However, only a few studies have demonstrated the involvement of Sp1 in lung responses to hyperoxia. For example, hyperoxia-induced increase of Sp1/Sp3 binding is known to induce transcriptional upregulation of an oxidant stress-dependent gene, Na,K–adenosine triphosphatase, in lung epithelial cells (48). Howlett and associates (49) demonstrated that inhaled nitric oxide (NO) protected against hyperoxia-induced apoptosis and inflammation in rat lungs, and this protection may be attributed to NO-induced inhibition of transcription factors, including Sp1. The mechanisms through which the −336 polymorphism in *Nrf2* contributes to the differential susceptibility to the hyperoxic lung injury have not been identified. However, it could be postulated that the −336 site has higher affinity for Sp1 proteins (than do other Sp1 sites in the promoter), and loss of this crucial Sp1 site may confer dysregulation of downstream hyperoxia-responsive genes. This, in turn, could lead to decreased lung injury or increased protection in the resistant C3 strain. We are conducting *in vitro* studies to resolve the role of −336 polymorphism in the differential sensitivity to hyperoxic lung injury. Together with the differential expression of constitutive and induced *Nrf2* mRNA levels in B6 and C3 mice and the results from functional analysis of *Nrf2* using gene-targeted mice (22), these observations provide strong supportive evidence for the importance of this candidate gene in differential susceptibility to hyperoxic lung injury.

Composite interval mapping analyses demonstrated that there was no interaction between *Hsl1* and *Hsl2* for cellular and hyperpermeability phenotypes. The minor QTL on chromosome 3 (*Hsl2*) includes a number of candidate genes, one of which is *NfkB*. NF-κB is known as a redox-sensitive transcription factor directly or indirectly activated by oxidative insult including hyperoxia (50, 51). Activated NF-κB induces proinflammatory cytokines including tumor necrosis factor (TNF)-α, interleukin (IL)-1β, IL-6, and IL-8 in pulmonary airways (50, 52). Importantly, Johnston and colleagues (16) demonstrated that, relative to the B6 strain, C3 mice had delayed expression of hyperoxia-inducible TNF-α, IL-1β, and IL-6 that was reflective of later injury. A recent *in vitro* study suggested that NF-κB contributes to hyperoxia-induced necrosis of alveolar cells (53). It is therefore postulated that NF-κB could be one of the genetic determinants that contribute to the increased susceptibility of mice to oxygen toxicity.

The genetic linkage analyses provided strong evidence that *Hsl1* and *Hsl2* largely control hyperoxia-induced cellular and permeability response. To further test the hypothesis that different genetic mechanisms control these responses to hyperoxia, we applied linear regression analyses for these phenotypes from the F_2 cohort. We reasoned that if the phenotypes were mechanistically and genetically related, then hyperoxia-induced inflammatory and epithelial cell changes would be coinherited with hyperpermeability in segregant progeny of B6 and C3 mice. The cosegrega-

tion analyses indicated there was statistically significant correlation between epithelial cell and any of the inflammatory cell responses as well as among inflammatory cell responses. In contrast, no significant correlation was observed between protein and cell responses. These analyses suggest that similar genetic mechanisms control the cell response in lungs exposed to oxygen, but lung permeability change may be controlled by a different mechanism(s). The dissociation of inflammatory and hyperpermeability responses in the lung has been demonstrated by a number of studies with oxidants. For example, depletion of PMNs with anti-PMN antibodies (54) or induction of PMN infiltration (55) before exposure did not affect the magnitude of pulmonary hyperpermeability induced by ozone (O_3) in rodents. It was subsequently determined that O_3-induced lung cellular responses (i.e., epithelial injury and inflammation) but not lung hyperpermeability were mediated by *Tnf* (56). Further, O_3-induced lung hyperpermeability but not cellular inflammation is mediated via inducible NO synthase (57, 58).

In conclusion, results strongly support linkage of susceptibility to hyperoxic lung injury with *Hsl1* and *Hsl2*. Strain-specific variation in *Nrf2* mRNA expression and the promoter polymorphism that segregated with hyperoxic pulmonary phenotypes and informative SSLP marker genotypes on chromosome 2 support *Nrf2* as a susceptibility gene in hyperoxic lung injury. The current results provide new and important insights into the molecular mechanisms underlying oxygen toxicity in pulmonary airways. Further investigation of the *Hsls* should lead to improved strategies for the therapy of oxidant-mediated respiratory diseases.

Acknowledgments: The authors acknowledge the contribution of the NIEHS Center-supported Inhalation Facility toward completion of these studies. This work received grant support from the National Institutes of Health (HL-66109, HL-58122, HL-57142, CA-44530, ES-03819, and ES-09606) and the Environmental Protection Agency (R-826724).

References

1. Fridovich, I. 1978. The biology of oxygen radicals. *Science* 201:875–880.
2. Halliwell, B., J. M. Gutteridge, and C. E. Cross. 1992. Free radicals, antioxidants, and human disease: where are we now? *J. Lab. Clin. Med.* 119:598–620.
3. Freeman, B. A., M. K. Topolosky, and J. D. Crapo. 1982. Hyperoxia increases oxygen radical production in rat lung homogenates. *Arch. Biochem. Biophys.* 216:477–484.
4. Crapo, J. D., B. E. Barry, H. A. Foscue, and J. Shelburne. 1980. Structural and biochemical changes in rat lungs occurring during exposure to lethal and adaptive doses of oxygen. *Am. Rev. Respir. Dis.* 122:123–143.
5. Crapo, J. D. 1986. Morphologic changes in pulmonary oxygen toxicity. *Annu. Rev. Physiol.* 48:721–731.
6. Clerch, L. B., and D. J. Massaro. 1993. Tolerance of rats to hyperoxia. *J. Clin. Invest.* 91:499–508.
7. Clark, J. M., and C. J. Lambertsen. 1971. Pulmonary oxygen toxicity: a review. *Pharmacol. Rev.* 23:37–133.
8. Canada, A. T., L. A. Herman, and S. L. Young. 1995. An age-related difference in hyperoxia lethality: role of lung antioxidant defense mechanisms. *Am. J. Physiol. (Lung Cell. Mol. Physiol.)* 268:L539–L545.
9. Denke, S. M., and B. L. Fanburg. 1980. Normobaric oxygen toxicity of the lung. *N. Engl. J. Med.* 303:76–86.
10. Gonder, J. C., R. D. Proctor, and J. A. Will. 1985. Genetic differences in oxygen toxicity are correlated with cytochrome P-450 inducibility. *Proc. Natl. Acad. Sci. USA* 82:6315–6319.
11. Mansour, H., M. Levacher, E. Azoulay-Dupuis, J. Moreau, C. Marquetty, and M. Gougerot-Pocidalo. 1988. Genetic differences in response to pulmonary cytochrome P-450 inducers and oxygen toxicity. *J. Appl. Physiol.* 64:1376–1381.
12. Stenzel, J. D., S. E. Welty, A. E. Benzick, E. O. Smith, C. V. Smith, and T. N. Hansen. 1993. Hyperoxic lung injury in Fischer-344 and Sprague-Dawley rats *in vivo. Free Radic. Biol. Med.* 14:531–539.
13. He, L., S. Chang, P. O. Montellano, T. J. Burke, and N. F. Voelkel. 1990. Lung injury in Fischer but not Sprague-Dawley rats after short term hyperoxia. *Am. J. Physiol. (Lung Cell. Mol. Physiol.)* 259:L451–L458.
14. Hudak, B. B., L. Zhang, and S. R. Kleeberger. 1993. Inter-strain variation in susceptibility to hyperoxic injury of murine airways. *Pharmacogenetics* 3:135–143.
15. Piedboeuf, B., C. J. Johnston, R. H. Watkins, B. B. Hudak, J. S. Lazo, M. G. Cherian, and S. Horowitz. 1994. Increased expression of tissue inhibitor of metalloproteinases (TIMP-1) and metallothionein in murine lungs after hyperoxic exposure. *Am. J. Respir. Cell Mol. Biol.* 10:123–132.
16. Johnston, C. J., B. R. Stripp, B. Piedbeouf, T. W. Wright, G. W. Mango, C. K. Reed, and J. N. Finkelstein. 1998. Inflammatory and epithelial responses in mouse strains that differ in sensitivity to hyperoxic injury. *Exp. Lung Res.* 24:189–202.
17. Itoh, K., T. Chiba, S. Takahashi, T. Ishii, K. Igarashi, Y. Katoh, T. Oyake, N. Hayashi, K. Satoh, I. Hatayama, M. Yamamoto, and Y. Nabeshima. 1997. A Nrf2/small Maf heterodimer mediates the induction of phase II detoxifying enzyme genes through antioxidant response elements. *Biochem. Biophys. Res. Commun.* 236:313–322.
18. Venugopal, R., and A. K. Jaiswal. 1996. Nrf1 and Nrf2 positively and c-Fos and Fra1 negatively regulate the human antioxidant response element-mediated expression of NAD(P)H:quinone oxidoreductase1 gene. *Proc. Natl. Acad. Sci. USA* 93:14960–14965.
19. Venugopal, R., and A. K. Jaiswal. 1998. Nrf2 and Nrf1 in association with Jun proteins regulate antioxidant response element-mediated expression and coordinated induction of genes encoding detoxifying enzymes. *Oncogene* 17:3145–3156.
20. Xie, T., M. Belinsky, Y. Xu, and A. K. Jaiswal. 1995. ARE- and TRE-mediated regulation of gene expression: response to xenobiotics and antioxidants. *J. Biol. Chem.* 270:6894–6900.
21. Jeyapaul, J., and A. K. Jaiswal. 2000. Nrf2 and c-Jun regulation of antioxidant response element (ARE)-mediated expression and induction of gamma-glutamylcysteine synthetase heavy subunit gene. *Biochem. Pharmacol.* 59:1433–1439.
22. Cho, H., A. E. Jedlicka, S. P. M. Reddy, T. W. Kensler, M. Yamamoto, L. Zhang, and S. R. Kleeberger. Role of NRF2 in protection against hyperoxic lung injury in mice. *Am. J. Respir. Cell Mol. Biol.* (In press)
23. Bradford, M. M. 1976. A rapid and sensitive method for the quantitation of microgram quantities of protein utilizing the principle of protein-dye binding. *Anal. Biochem.* 72:248–254.
24. Saltini, C., A. J. Hance, V. J. Ferrans, F. Basset, P. B. Bitterman, and R. G. Crystal. 1984. Accurate quantitation of cells recovered by bronchoalveolar lavage. *Am. Rev. Respir. Dis.* 130:650–658.
25. Ohtsuka, Y., K. J. Brunson, A. E. Jedlicka, W. Mitzner, R. W. Clarke, L. Zhang, S. M. Eleff, and S. R. Kleeberger. 2000. Genetic linkage analysis of susceptibility to particle exposure in mice. *Am. J. Respir. Cell Mol. Biol.* 22:574–581.
26. Silver, L. M. 1995. Mouse Genetics. Oxford University Press, New York.
27. Lander, E. S., and D. Botstein. 1989. Mapping Mendelian factors underlying quantitative traits using RFLP linkage maps. *Genetics* 121:185–199.
28. Manly, K. F., and J. M. Olson. 1999. Overview of QTL mapping software and introduction to Map Manager QT. *Mamm. Genome* 10:327–334.
29. Churchill, G. A., and R. W. Doerge. 1994. Empirical threshold values for quantitative trait mapping. *Genetics* 138:963–971.
30. Lander, E., and L. Kruglyak. 1995. Genetic dissection of complex traits: guidelines for interpreting and reporting linkage results. *Nat. Genet.* 11:241–247.
31. Chomczynski, P., and N. Sacchi. 1987. Single-step method of RNA isolation by acid guanidinium thiocyanate-phenol-chloroform extraction. *Anal. Biochem.* 162:156–159.
32. Chan, K., R. Lu, J. C. Chang, and Y. W. Kan. 1996. Nrf2, a member of NFE2 family of transcription factors, is not essential for murine erythropoiesis, growth and development. *Proc. Natl. Acad. Sci. USA* 93:13943–13948.
33. Clark, D. A., L. G. Pincus, M. Oliphant, C. Hubbell, R. P. Oates, and F.R. Davey. 1982. HLA-A2 and chronic lung disease in neonates. *JAMA* 248:1868–1869.
34. Parker, R. A., D. P. Lindstrom, and R. B. Cotton. 1996. Evidence from twin study implies possible genetic susceptibility to bronchopulmonary dysplasia. *Semin. Perinatol.* 20:206–209.
35. Alam, J., D. Stewart, C. Touchard, S. Boinapally, A. M. Choi, and J. L. Cook. 1999. Nrf2, a cap'n'collar transcription factor, regulates induction of the heme oxygenase-1 gene. *J. Biol. Chem.* 274:26071–26078.
36. Chan, K., and Y. W. Kan. 1999. Nrf2 is essential for protection against acute pulmonary injury in mice. *Proc. Natl. Acad. Sci. USA* 96:12731–12736.
37. Guyton, K. Z., J. A. Thompson, and T. W. Kensler. 1993. Role of quinone methide in the in vitro toxicity of the skin tumor promoter butylated hydroxytoluene hydroperoxide. *Chem. Res. Toxicol.* 6:731–738.
38. Enomoto, A., K. Itoh, E. Nagayoshi, J. Haruta, T. Kimura, T. O'Connor, T. Harada, and M. Yamamoto. 2001. High sensitivity of Nrf2 knockout mice to acetaminophen hepatotoxicity associated with decreased expression of ARE-regulated drug metabolizing enzymes and antioxidant genes. *Toxicol. Sci.* 59:169–177.
39. Ramos-Gomez, M., M. Kwak, P. M. Dolan, K. Itoh, M. Yamamoto, P. Talalay, and T. W. Kensler. 2001. Sensitivity to carcinogenesis is increased and chemoprotective efficacy of enzyme inducers is lost in *nrf2* transcription factor-deficient mice. *Proc. Natl. Acad. Sci. USA* 98:3410–3415.
40. Folz, R. J., A. M. Abushamaa, and H. B. Suliman. 1999. Extracellular superoxide dismutase in the airways of transgenic mice reduces inflammation and attenuates lung toxicity following hyperoxia. *J. Clin. Invest.* 103:1055–1066.

41. Danel, C., S. C. Erzurum, P. Prayssac, N. T. Eissa, R. G. Crystal, P. Herve, B. Baudet, M. Mazmanian, and P. Lemarchand. 1998. Gene therapy for oxidant injury-related diseases: adenovirus-mediated transfer of superoxide dismutase and catalase cDNAs protects against hyperoxia but not against ischemia-reperfusion lung injury. *Hum. Gene Ther.* 9:1487–1496.
42. O'Brien, P. J. 1991. Molecular mechanisms of quinone cytotoxicity. *Chem. Biol. Interact.* 80:1–41.
43. Fahey, J. W., and P. Talalay. 1999. Antioxidant functions of sulforaphane: a potent inducer of Phase II detoxication enzymes. *Food Chem. Toxicol.* 137:973–979.
44. Whitney, P. L., and L. Frank. 1993. Does lung NAD(P)H:quinone reductase (DT-diaphorase) play an antioxidant enzyme role in protection from hyperoxia? *Biochim. Biophys. Acta.* 1156:275–282.
45. Rahman, I., A. Bel, B. Mulier, M. F. Lawson, D. J. Harrison, W. Macnee, and C. A. Smith. 1996. Transcriptional regulation of gamma-glutamylcysteine synthetase-heavy subunit by oxidants in human alveolar epithelial cells. *Biochem. Biophys. Res. Commun.* 229:832–837.
46. Otterbein, L. E., J. K. Kolls, L. L. Mantell, J. L. Cook, J. Alam, and A. M. Choi. 1999. Exogenous administration of heme oxygenase-1 by gene transfer provides protection against hyperoxia-induced lung injury. *J. Clin. Invest.* 103:1047–1054.
47. Ishii, T., K. Itoh, S. Takahashi, H. Sato, T. Yanagawa, Y. Katoh, S. Bannai, and M. Yamamoto. 2000. Transcription factor Nrf2 coordinately regulates a group of oxidative stress-inducible genes in macrophages. *J. Biol. Chem.* 275:16023–16029.
48. Wendt, C. H., G. Greg, R. Sharma, Y. Zhuang, W. Deng, and D. H. Ingbar. 2000. Up-regulation of Na,K-ATPase β_1 transcription by hyperoxia is mediated by Sp1/Sp3 binding. *J. Biol. Chem.* 275:41396–41404.
49. Howlett, C. E., J. S. Hutchison, J. P. Veinot, A. Chiu, P. Merchant, and H. Fliss. 1999. Inhaled nitric oxide protects against hyperoxia-induced apoptosis in rat lungs. *Am. J. Physiol. (Lung Cell Mol. Physiol).* 277:L596–L605.
50. Shea, L. M., C. Beehler, M. Schwartz, R. Shenkar, R. Tuder, and E. Abraham. 1996. Hyperoxia activates NF-kappaB and increases TNF-alpha and IFN-gamma gene expression in mouse pulmonary lymphocytes. *J. Immunol.* 157:3902–3908.
51. Janssen-Heininger, Y. M., I. Macara, and B. T. Mossman. 1999. Cooperativity between oxidants and tumor necrosis factor in the activation of nuclear factor (NF)-kappaB: requirement of Ras/mitogen-activated protein kinases in the activation of NF-kappaB by oxidants. *Am. J. Respir. Cell Mol. Biol.* 20:942–952.
52. Blackwell, T. S., and J. W. Christman. 1997. The role of nuclear factor κB in cytokine gene regulation. *Am. J. Respir. Cell Mol. Biol.* 17:3–9.
53. Li, Y., W. Zhang, L. L. Mantell, J. A. Kazzaz, A. M. Fein, and S. Horowitz. 1997. Nuclear factor-kappa B is activated by hyperoxia but does not protect from cell death. *J. Biol. Chem.* 272:20646–20649.
54. Kleeberger, S. R., and B. B. Hudak. 1992. Acute ozone-induced change in airway permeability: the role of infiltrating leukocytes. *J. Appl. Physiol.* 72:670–676.
55. Reinhart, P. G., D. J. Bassett, and D. K. Bhalla. 1998. The influence of polymorphonuclear leukocytes on altered pulmonary epithelial permeability during ozone exposure. *Toxicology* 127:17–28.
56. Cho, H.-Y., A. E. Jedlicka, L.-Y. Zhang, and S. R. Kleeberger. 2001. Ozone-induced pulmonary inflammation and hyperreactivity are mediated via 55 and 75 kDa receptors for tumor necrosis factor receptor-α. *Am. J. Physiol. Lung Cell. Mol. Physiol.* 280:L537–L546.
57. Kleeberger, S. R., S. P. M. Reddy, L.-Y. Zhang, and A. E. Jedlicka. 2000. Genetic susceptibility to ozone-induced lung hyperpermeability: role of the toll-like receptor 4 (*Tlr4). Am. J. Respir. Cell Mol. Biol.* 22:620–627.
58. Kleeberger, S. R., S. P. M. Reddy, L.-Y. Zhang, H.-Y. Cho, and A. E. Jedlicka. 2001. Toll-like receptor 4 (*Tlr4*) mediates ozone-induced murine lung hyperpermeability via inducible nitric oxide synthase. *Am. J. Physiol. (Lung Cell Mol. Physiol.)* 280:L326–L333.